Ectopic FVIII expression and misfolding in hepatocytes as a potential cause of human hepatocellular carcinoma

Ruishu Deng[1], Audrey Kapelanski-Lamoureux[2], Zu-hua Gao[3], Anthoula Lazaris[4], Lisa Giles[5], Jyoti Malhotra[6], Jing Yong[1], Peter Metrakos[7], Randal J Kaufman[1,8,*]

[1] Degenerative Diseases Program, SBP Medical Discovery Institute, La Jolla, United States

[2] Department of Anatomy and Cell Biology, McGill University, Cancer Research Program, Research Institute of the McGill University Health Centre, Montreal, Quebec Canada

[3] Department of Pathology, McGill University Health Centre, Montreal, Quebec, Canada

[4] Cancer Research Program, Research Institute of the McGill University Health Centre, Montreal, Quebec Canada

[5] Not affiliated with any institution

[6] Sarepta Therapeutics, Boston MA, United States

[7] Department of Surgery, McGill University;Cancer Research Program, Research Institute of the McGill University Health Centre,Montreal, Quebec Canada

[8] Department of Pharmacology, University of California, San Diego, La Jolla, United States

***:** Corresponding Author:

Randal J. Kaufman: rkaufman@sbpdiscovery.org

Abstract

Clotting Factor VIII (**FVIII**) is the protein deficient in hemophilia A (**HA**), an X chromosome-linked bleeding disorder affecting 24.6 per 100,000 males at birth. Scientists and clinical physicians have been striving hard to find a cure for this disease. Presently, HA therapy involves prophylactic infusion of plasma-derived or recombinant-derived FVIII. Recent clinical studies have reported success using recent adeno-associated-virus (**AAV**) vector mediated delivery of a FVIII gene. FVIII is a 330 kDa glycoprotein comprised of three domains (A1-A2-B-A3-C1-C2). The B domain is dispensable and B domain-deleted (**BDD**) FVIII is used in the clinic as an effective protein replacement therapy for HA. Previously, we observed that hydrodynamic tail vein injection of the BDD-FVIII vector resulted in FVIII aggregation and endoplasmic reticulum (**ER**) stress in murine livers. Additionally, mice that were exposed to transient ER stress and then fed a high fat diet (**HFD**) for 9 months developed hepatocellular carcinoma (**HCC**). Therefore, we deduced that ectopic transient expression of FVIII in hepatocytes of mice with subsequent HFD feeding may also develop HCC. Here, we tested hepatocyte expression of two BDD-FVIII variants *in vivo*. BDD-FVIII aggregates in the ER and induces hepatocyte apoptosis, and N6-FVIII is more efficiently folded and secreted from the ER and causes less hepatocyte apoptosis. We performed tail vein injections of vectors directing expression of BDD-FVIII or N6-BDD to hepatocytes of 6-week old mice. One week after injection, mice were fed 60% HFD for 65 weeks. We found that 50% of mice that received N6-BDD developed liver tumors; in contrast, 90% of mice given BDD-FVIII developed liver tumors. Of the mice injected with BDD-FVIII, 30% developed carcinomas and 60% developed adenomas. Similar masses were not observed in mice that received empty vector. These

findings raise concerns about the safety of long-term ectopic expression of FVIII in hepatocytes during FVIII gene therapy

Introduction

Clotting Factor VIII (**FVIII**) protein deficiency causes hemophilia A (**HA**), an X chromosome-linked bleeding disorder affecting 24.6 per 100,000 males at birth (Srivastava et al., 2020). Prophylactic administration of recombinant FVIII as a protein replacement therapy has significantly reduced morbidity and mortality resulting from HA. However, ectopic FVIII expression in mammalian cells, mainly in Chinese Hamster Ovary (**CHO**) cells (Kaufman, 1989), is inefficient, partly due to FVIII misfolding, protein aggregate formation and impaired trafficking from the ER (Poothong et al., 2020). Furthermore, FVIII protein replacement therapy is significantly hampered due to low and variable production resulting in increased cost and limited availability; also, reports of inhibitory anti-FVIII antibodies that had developed in a significant cohort of patients (Gouw et al., 2013). However, HA gene therapy clinical studies using adeno-associate-viral (**AAV**) vector-mediated FVIII gene delivery have proven successful, partly due to low level of FVIII expression after the 1st year of administration (Pierce, 2020; Pierce et al., 2020; Sheridan, 2020). Therefore, there is an urgent need to understand the mechanism underlying inefficient FVIII production and secretion both in an engineered bio-production system, and importantly, in *in vivo* clinical settings (Pierce, 2020; Pierce et al., 2020; Sheridan, 2020).

FVIII is a 330 kDa glycoprotein comprised of three domains (A1-A2-B-A3-C1-C2)(Pittman et al., 1994). The amino acid sequences in FVIII's A and C domains are highly conserved

between species, whereas the amino acid sequence of the large B domain, encoded by a single 3kb exon, is not conserved. In addition, the B domain bears an unusually large number (18) of N-linked oligosaccharides. The B domain is dispensable for secretion of functional FVIII activity (Pittman et al., 1993). In fact, B domain-deleted (**BDD**) FVIII is used in the clinic as effective protein replacement therapy for HA (Lusher et al., 2003; Lusher and Roth, 2005; Rangarajan et al., 2017), and used exclusively in HA gene therapy due to the packaging capacity of the AAV genome, which is <5kb (Grimm and Kay, 2003). In contrast, we reported that a slightly bigger FVIII molecule with a partial B domain deletion (**FVIII-N6**), which retains an additional 226 aa with 6 N-linked glycosylation sites from the B domain), is secreted 10-fold more efficiently than full length FVIII and BDD (Malhotra et al., 2008), presumably because of increased engagement with the lectin chaperone machinery of the cell (Cunningham et al., 2003; Moussalli et al., 1999; Zhang et al., 2005; Zhang et al., 2011). In addition to the desirable high secretion efficiency FVIII-N6 exhibits reduced cellular toxicity, as measured by markers of the unfolded protein response (**UPR**) and systemic inflammatory response (**INF**), and levels of reactive oxygen species (**ROS**), among others (**Figure 1**) (Malhotra et al., 2008; Miao et al., 2004; Rutkowski et al., 2008; Zhang et al., 2006).

In the current study, by using a hydrodynamic injection-based gene delivery method, we directed expression of FVIII-N6 and FVIII-BDD to livers of 6 week old mice. One week after the injection, mice were fed a 60% High Fat Diet (**HFD**) for 65 weeks. We found that 50% of mice given FVIII-N6 developed liver tumors; in contrast, 90% of mice given FVIII-BDD developed liver tumors. Specifically, within the FVIII-BDD-injected mice, 30% developed carcinomas and 60% developed adenomas. These results further confirm our

previous observation that ER stress combined with hyper nutrition induce HCC development. Importantly, it serves as a forewarning for ongoing clinical trials using FVIII-BDD in HA gene therapy to closely monitor the liver status of recruited patients during treatment.

Results

Hydrodynamic injection of FVIII-BDD vector causes hepatocellular carcinoma

Hydrodynamic injection is an efficient way of exogenous gene expression, with target gene expression largely detected in the liver (Liu et al., 1999). Using this technique, we have confirmed expression of exogenous FVIII in hepatocytes of mice injected with pMT-BDD and pMT-N6 (Malhotra et al., 2008). Of note, ER stress was also observed in hepatocytes of mice injected with pMT-BDD (Malhotra et al., 2008). In a separate report by our lab, ER stress together with hyper nutrition was shown to trigger HCC development (Nakagawa et al., 2014). Following these observations, 6-week old C57BL/6J mice were injected with pMT-BDD, pMT-N6 and pMT, empty vector, and then fed a 60% HFD beginning one week after injection. After 65 weeks of HFD feeding, mice were sacrificed, and liver tissue was harvested for evaluation of tumor formation (**Fig 2A**). Following strict diagnosis standards, H.E. staining slides were evaluated independently by three different clinical pathologists from the Mayo Clinic (USA) and McGill University Department of Pathology (Canada). Immunohistochemistry staining of glutamine synthetase and CD34 were also performed to assist the diagnosis. Interestingly, we did not find any tumor formation in the 8 mice injected with pMT vector. We did observe tumor formation in 9 out of 10 mice (90%) given pMT-BDD, which was significantly higher than that in mice that

received pMT-N6. (**Fig. 2B**, $p<0.0001$, Chi-square test). Reports of the three independent pathologists state that 6 of the 9 pMT-BDD-injected mice developed adenomas and 3 developed adenocarcinomas (**Fig. 2C**). Out of the 3 adenocarcinomas, 2 cases were strongly positive for glutamine synthetase staining (**Fig. 2D**) and 1 of them displayed a patchy strong CD34-positive staining (**Fig. 2D**), further confirming the malignancy (Cui et al., 1996; Wasfy and Shams Eldeen, 2015). Collectively, these results indicate that exogenous expression of pMT-BDD caused hepatocyte adenocarcinomas in mice placed on an extended 60% HFD.

Ectopic FVIII expression via hydrodynamic tail vein injection causes protein aggregation in mouse livers

We next sought to investigate whether the effect from FVIII gene delivery to hepatocytes is associated with BDD/N6's tendency to form protein aggregates *in vivo.* We addressed this by monitoring aggregates using Thioflavin-S staining after gene delivery of BDD and 226/N6 via hydrodynamic tail vein injections. The livers of BDD-injected mice showed significantly more aggregate formation than pMT-N6 injected mice livers, evidenced by colocalization of Thioflavin-S staining with anti-FVIII immunostaining (**Figure 3**).

FVIII aggregates begin to resolve as early as 30 minutes following energy repletion

For a potential molecular mechanism to explain the difference in biological effects resulting from ectopic expression of BDD versus N6 variants that we observed *in vivo*, we examined CHO cells that stably expressed either BDD-FVIII, or N6-FVIII. Although stably transfected CHO cells express 226/N6 at a greater level than BDD (10 U/ml vs. 1 U/ml), less aggregates were observed under untreated conditions, consistent with the increased secretion efficiency (**Figure 4**). Following energy depletion via 2DG treatment, FVIII

aggregates accumulated in CHO cells that stably expressed wtFVIII (~500mU/ml/day, data not shown) (Poothong et al., 2020), BDD (~1U/ml/day) and 226/N6 (~10U/ml/day) (**Figure 4**). After changing to normal media, FVIII aggregates began to disappear as early as 30 min, in a manner that did not require *de novo* protein synthesis, as addition of a protein synthesis inhibitor cycloheximide (**CHX**) to the recovery media had no effect.

Pulse-chase analyses demonstrate FVIII aggregates can be secreted from the cell

Pulse-chase analyses confirmed that energy depletion retains FVIII within the cell, and that, upon energy repletion, intracellular aggregated FVIII is lost and, remarkably, is recovered in the medium. A parallel experiment testing the activity of FVIII in media treated using the same conditions as the pulse chase assay demonstrated that the secreted FVIII is functional (**Fig. 5**). Increasing amounts of functional FVIII appeared in the media as early as 30 minutes following energy repletion. Although the amount of FVIII that is secreted following energy repletion appears unaffected by the addition of CHX to the repletion media, the level of active FVIII secreted does seem CHX sensitive. However, even in the presence of CHX, active FVIII is still secreted at greater levels than under energy depletion conditions, suggesting that at least some of the active FVIII secreted was most likely released from intracellular aggregates.

Acknowledgment

This work was supported by NIH grants CA198103, and DK113171 to R.J.K..

Material and Method

Mice

Male C57BL/6J mice were purchased from Jackson Laboratory and maintained at the Sanford-Burnham-Prebys Medical Discovery Institute animal facility. Mice were euthanized by CO_2 inhalation for liver harvest. All animal protocols were reviewed and approved by the Institutional Animal Care and Use Committee at the SBP Medical Discovery Institute.

Hydrodynamics-based delivery of plasmid and HCC development

The expression vectors for pMT-BDD and pMT-N6 were previously described(Miao et al., 2004). Six-week old mice were used for these experiments. Hydrodynamic tail vein injection was performed according to previous publications (Liu et al., 1999; Malhotra et al., 2008). In summary, 100ug plasmid was diluted in 2.5ml saline and injected into the mouse through the tail vein. One week after the injection, mice were given 60% HFD for 65 weeks after which their livers were harvested for tumor evaluation.

Histology and Immunohistochemistry staining

Livers were fixed in 10% neutral-buffered formalin for about 48 hours and sent to histology core for paraffin embedding and section. FFPE sections were used for hematoxylin and eosin (H&E) and IHC staining. IHC staining was performed as described previously (Nakagawa et al., 2014). Briefly, slides were dewaxed and heat induced antigen retrieval was performed in Sodium Citrate pH 6.0. Slides were incubated with primary antibodies against glutamine synthetase (abcam, cat #: ab176562, 1:1000) or CD35 (abcam, cat #: ab81289, 1:2500) overnight at 4C, followed by HRP-labeled secondary antibodies (DAKO

Cat #, K400311) and then visualized with DAB (brown staining). Thioflavin S staining was performed as we previously described (Poothong et al., 2020).

Materials for cellular and molecular biology

Anti-factor VIII heavy chain monoclonal antibody coupled to Sepharose CL-4B was obtained from Baxter. FVIII-deficient and normal pooled human plasma were obtained from George King Biomedical (Overland Park, KS). Activated partial thromboplastin (automated aPTT reagent) and $CaCl_2$ were purchased from General Diagnostics Organon Teknika (Durham, NC). Dulbecco modified Eagle medium (DMEM), glucose-free DMEM, alpha-modified essential medium (alpha-MEM), cysteine/methionine-free DMEM, and fetal bovine serum (FBS) were purchased from Gibco BRL. FVIII:C-EIA was purchased from Affinity Biologicals. Anti-β-actin antibody, 3-methyladenine, 2-deoxy-D-glucose, and sodium azide were obtained from Sigma Aldrich. Anti-FVIII antibody (GMA012) was obtained from Green Mountain. [^{35}S]-Methionine/Cysteine was obtained from MP Biologicals. Mouse and rabbit horseradish peroxidase conjugated secondary antibodies, Prolong Antifade Gold and Complete Protease Inhibitor Cocktail were obtained from Promega. Supersignal West Pico ECL was obtained from Thermo. Mouse FAB fragments, Dylight 549 conjugated anti-mouse fab fragments and Texas-Red conjugated anti-mouse secondary were obtained from Jackson Immunoresearch.

Energy depletion and repletion

For depletion of intracellular ATP, cells were treated with ATP-depleting medium (glucose-free DMEM containing 20 mM 2-deoxy-D-glucose and 10 mM sodium azide) for 2 h. To replete intracellular ATP, ATP-depleting medium was removed and replaced with

normal media for indicated time. Cycloheximide at a final concentration of 10 mg/mL was added to the repletion media where indicated.

Factor VIII activity and antigen analysis

FVIII activity was measured by a 1-stage aPTT clotting assay on an MLA Electra 750 fibrinometer (Medical Laboratory Automation, Pleasantville, NY) by reconsititution of human FVIII-deficient plasma. The FVIII plasma standard was FACT plasma (normal pooled plasma) from George King Biomedical. FVIII antigen was quantified by an anti-FVIII sandwich enzyme-linked immunosorbent assay (ELISA) method using the Affinity Biologicals FVIII:C-EIA commercial kit according to the manufacturers' instructions.

Metabolic labeling

Cells were subcultured 24 h prior to labeling in 60 mm dishes (approximately 106 cells/plate) and were 80% confluent at the time of labeling. Cells were washed twice in cys/met free DMEM and incubated in cys/met-free DMEM for 10 min prior to labeling. Cells were labeled in 0.5 ml cys/met free DMEM containing 100 mCi/mL (BDD and 226/N6) or 300 mCi/mL (10A1) for 20 min and chased for indicated times with conditioned medium (either ATP-depleting medium or normal medium) containing excess unlabeled cysteine and methionine and 10 mg/ml aprotinin. For depletion/repletion conditions, ATP-depleting medium was removed after 2 h and replaced with normal medium containing excess unlabeled cysteine and methionine and aprotinin as above. At the end of the chase period, conditioned media was collected. Cells were rinsed three times in phosphate buffered saline (PBS) and harvested in 1 ml lysis buffer [50 mM Tris-HCl, pH 7.4, 150 mM NaCl, 0.1% (v/v) Triton X-100, and 1% (v/v) IGEPAL] containing Complete Protease Inhibitor Cocktail and 1 mM phenylmethylsulfonyl fluoride. Lysates were

incubated on ice 30 min, followed by centrifugation at 15,000 x g for 10 min. Post-nuclear supernatant was then assayed for protein content using BCA assay (Bio-Rad). Equal amounts of protein and corresponding amounts of media were subjected to FVIII immunoprecipitation using anti-FVIII coupled Sepharose CL-4B beads at 4 ˚C overnight. Immunoprecipitates were washed 4 times with lysis buffer and proteins were separated by SDS-PAGE on a 6% polyacrylamide gel. Immunoprecipitated proteins were visualized by autoradiography and band intensities were quantified using ImageQuant.

Statistical Analyses

Statistical analyses were performed using GraphPad Prism 9. Chi-square test was used for comparing of tumor incidence between pMT BDD and pMT N6 groups. A p value < 0.05 was regarded as statistically significant.

Reference

Cui, S., Hano, H., Sakata, A., Harada, T., Liu, T., Takai, S., and Ushigome, S. (1996). Enhanced CD34 expression of sinusoid-like vascular endothelial cells in hepatocellular carcinoma. Pathol Int *46*, 751-756.

Cunningham, M.A., Pipe, S.W., Zhang, B., Hauri, H.P., Ginsburg, D., and Kaufman, R.J. (2003). LMAN1 is a molecular chaperone for the secretion of coagulation factor VIII. J Thromb Haemost *1*, 2360-2367.

Gouw, S.C., van der Bom, J.G., Ljung, R., Escuriola, C., Cid, A.R., Claeyssens-Donadel, S., van Geet, C., Kenet, G., Makipernaa, A., Molinari, A.C.*, et al.* (2013). Factor VIII products and inhibitor development in severe hemophilia A. N Engl J Med *368*, 231-239.

Grimm, D., and Kay, M.A. (2003). From virus evolution to vector revolution: use of naturally occurring serotypes of adeno-associated virus (AAV) as novel vectors for human gene therapy. Curr Gene Ther *3*, 281-304.

Kaufman, R.J. (1989). Genetic engineering of factor VIII. Nature *342*, 207-208.
Liu, F., Song, Y., and Liu, D. (1999). Hydrodynamics-based transfection in animals by systemic administration of plasmid DNA. Gene Ther *6*, 1258-1266.

Lusher, J.M., Lee, C.A., Kessler, C.M., Bedrosian, C.L., and ReFacto Phase 3 Study, G. (2003). The safety and efficacy of B-domain deleted recombinant factor VIII concentrate in patients with severe haemophilia A. Haemophilia *9*, 38-49.

Lusher, J.M., and Roth, D.A. (2005). The safety and efficacy of B-domain deleted recombinant factor VIII concentrates in patients with severe haemophilia A: an update. Haemophilia *11*, 292-293.

Malhotra, J.D., Miao, H., Zhang, K., Wolfson, A., Pennathur, S., Pipe, S.W., and Kaufman, R.J. (2008). Antioxidants reduce endoplasmic reticulum stress and improve protein secretion. Proc Natl Acad Sci U S A *105*, 18525-18530.

Miao, H.Z., Sirachainan, N., Palmer, L., Kucab, P., Cunningham, M.A., Kaufman, R.J., and Pipe, S.W. (2004). Bioengineering of coagulation factor VIII for improved secretion. Blood *103*, 3412-3419.

Moussalli, M., Pipe, S.W., Hauri, H.P., Nichols, W.C., Ginsburg, D., and Kaufman, R.J. (1999). Mannose-dependent endoplasmic reticulum (ER)-Golgi intermediate compartment-53-mediated ER to Golgi trafficking of coagulation factors V and VIII. J Biol Chem *274*, 32539-32542.

Nakagawa, H., Umemura, A., Taniguchi, K., Font-Burgada, J., Dhar, D., Ogata, H., Zhong, Z., Valasek, M.A., Seki, E., Hidalgo, J.*, et al.* (2014). ER stress cooperates with hypernutrition to trigger TNF-dependent spontaneous HCC development. Cancer Cell *26*, 331-343.

Pierce, G.F. (2020). Gene Therapy for Hemophilia: Are Expectations Matching Reality? Mol Ther *28*, 2097-2098.

Pierce, G.F., Kaczmarek, R., Noone, D., O'Mahony, B., Page, D., and Skinner, M.W. (2020). Gene therapy to cure haemophilia: Is robust scientific inquiry the missing factor? Haemophilia *26*, 931-933.

Pittman, D.D., Alderman, E.M., Tomkinson, K.N., Wang, J.H., Giles, A.R., and Kaufman, R.J. (1993). Biochemical, immunological, and in vivo functional characterization of B-domain-deleted factor VIII. Blood *81*, 2925-2935.

Pittman, D.D., Marquette, K.A., and Kaufman, R.J. (1994). Role of the B domain for factor VIII and factor V expression and function. Blood *84*, 4214-4225.

Poothong, J., Pottekat, A., Siirin, M., Campos, A.R., Paton, A.W., Paton, J.C., Lagunas-Acosta, J., Chen, Z., Swift, M., Volkmann, N.*, et al.* (2020). Factor VIII exhibits chaperone-dependent and glucose-regulated reversible amyloid formation in the endoplasmic reticulum. Blood *135*, 1899-1911.

Rangarajan, S., Walsh, L., Lester, W., Perry, D., Madan, B., Laffan, M., Yu, H., Vettermann, C., Pierce, G.F., Wong, W.Y.*, et al.* (2017). AAV5-Factor VIII Gene Transfer in Severe Hemophilia A. N Engl J Med *377*, 2519-2530.

Rutkowski, D.T., Wu, J., Back, S.H., Callaghan, M.U., Ferris, S.P., Iqbal, J., Clark, R., Miao, H., Hassler, J.R., Fornek, J.*, et al.* (2008). UPR pathways combine to prevent hepatic steatosis caused by ER stress-mediated suppression of transcriptional master regulators. Dev Cell *15*, 829-840.

Sheridan, C. (2020). A reprieve from hemophilia A, but for how long? Nat Biotechnol *38*, 1107-1109.

Srivastava, A., Santagostino, E., Dougall, A., Kitchen, S., Sutherland, M., Pipe, S.W., Carcao, M., Mahlangu, J., Ragni, M.V., Windyga, J.*, et al.* (2020). WFH Guidelines for the Management of Hemophilia, 3rd edition. Haemophilia *26 Suppl 6*, 1-158.

Wasfy, R.E., and Shams Eldeen, A.A. (2015). Roles of Combined Glypican-3 and Glutamine Synthetase in Differential Diagnosis of Hepatocellular Lesions. Asian Pac J Cancer Prev *16*, 4769-4775.

Zhang, B., Kaufman, R.J., and Ginsburg, D. (2005). LMAN1 and MCFD2 form a cargo receptor complex and interact with coagulation factor VIII in the early secretory pathway. J Biol Chem *280*, 25881-25886.

Zhang, B., Zheng, C., Zhu, M., Tao, J., Vasievich, M.P., Baines, A., Kim, J., Schekman, R., Kaufman, R.J., and Ginsburg, D. (2011). Mice deficient in LMAN1 exhibit FV and FVIII deficiencies and liver accumulation of alpha1-antitrypsin. Blood *118*, 3384-3391.

Zhang, K., Shen, X., Wu, J., Sakaki, K., Saunders, T., Rutkowski, D.T., Back, S.H., and Kaufman, R.J. (2006). Endoplasmic reticulum stress activates cleavage of CREBH to induce a systemic inflammatory response. Cell *124*, 587-599.

Ectopic FVIII expression and misfolding in hepatocytes as a potential cause of human hepatocellular carcinoma

Ruishu Deng[1], Audrey Kapelanski-Lamoureux[2], Zu-hua Gao[3], Anthoula Lazaris[4], Lisa Giles[5], Jyoti Malhotra[6], Jing Yong[1], Peter Metrakos[7], Randal J Kaufman[1,8,*]

[1] Degenerative Diseases Program, SBP Medical Discovery Institute, La Jolla, United States

[2] Department of Anatomy and Cell Biology, McGill University, Cancer Research Program, Research Institute of the McGill University Health Centre, Montreal, Quebec Canada

[3] Department of Pathology, McGill University Health Centre, Montreal, Quebec, Canada

[4] Cancer Research Program, Research Institute of the McGill University Health Centre, Montreal, Quebec Canada

[5] Not affiliated with any institution

[6] Sarepta Therapeutics, Boston MA, United States

[7] Department of Surgery, McGill University;Cancer Research Program, Research Institute of the McGill University Health Centre,Montreal, Quebec Canada

[8] Department of Pharmacology, University of California, San Diego, La Jolla, United States

***:** Corresponding Author:

Randal J. Kaufman: rkaufman@sbpdiscovery.org

Figure 1. Hepatocyte responses to wtFVIII and BDD FVIII variants upon HTD delivery to mice.

FVIII secretion efficiency, activation of the UPR, activation of the systemic inflammatory response (**INF**), production of reactive oxygen species (**ROS**), induction of cell death, hepatic steatosis, the ability for BHA to prevent toxic responses and potential for HCC. ? = not studied. a1-3 = acidic regions.

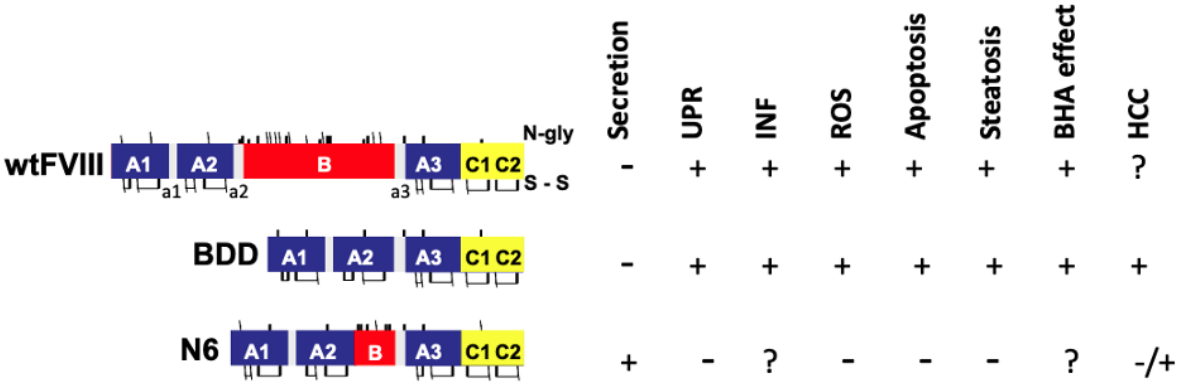

Figure 2. Hydrodynamic injection of pMT-BDD causes hepatocyte carcinoma in mice after HFD

WT C57BL/6 mice injected with plasmids, pMT-vector, pMT-N6, pMT-BDD were given a 60% HFD one week after the injection. After 65 weeks of HFD, livers were harvested for tumor evaluation. (**A**) Representative image of livers from the indicated groups. The black circles indicate tumors. (**B**) The incidence of tumor formation in the pMT-BDD group was higher than that in the pMT-N6 group. (**C**) Pie chart shows the percentage of carcinoma and adenoma in pMT-BDD group. (**D**) Representative H&E and IHC staining of glutamine synthetase and CD34 in liver sections from two carcinoma cases caused by pMT-BDD.

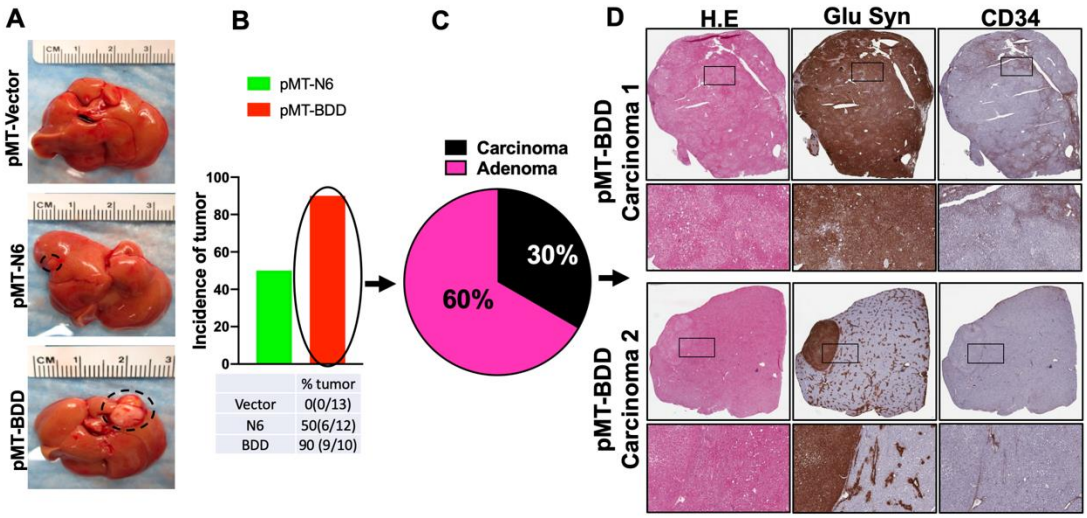

Figure 3: Ectopic FVIII expression causes protein aggregation in liver
WT *C57BL/6* mice received plasmids pMT-vector, pMT-N6, or pMT-BDD via hydrodynamic tail vein injection. Mice were sacrificed, with their livers fixed and stained with anti-FVIII antibody and thioflavin-S (Thio-S) for analysis by immunofluorescence microscopy.

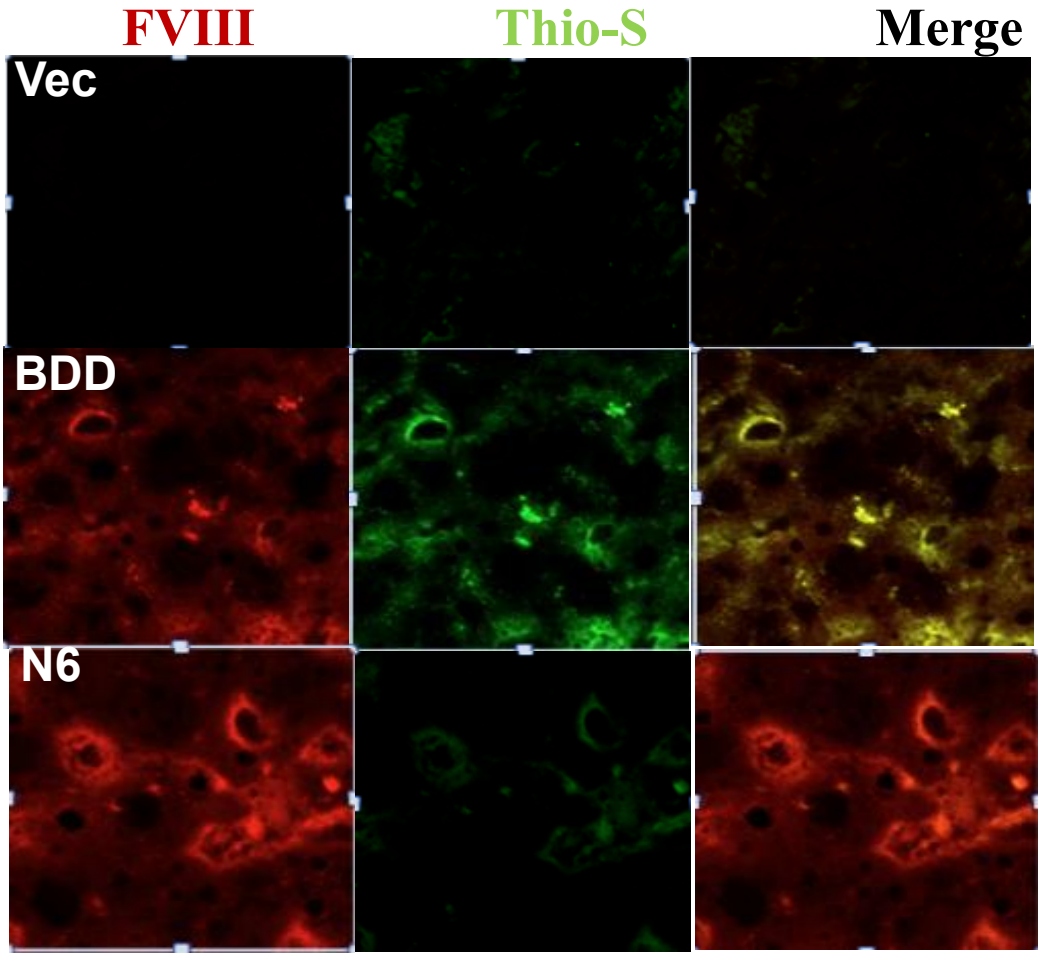

Figure 4. Aggregates induced by energy depletion begin to resolve as early as 30 minutes following energy repletion.

CHO cells that express wtFVIII, BDD or 226/N6 were treated with either normal media or glucose-free media containing 10 mM 2DG and 20 mM azide (2DG). After 2 hr, cells were harvested or allowed to recover in complete media for the indicated time, or complete media with 10 μg/ml CHX. Cell lysates were filtered through nitrocellulose (left) or cellulose acetate (right) and probed with α-FVIII or α-β-actin antibodies.

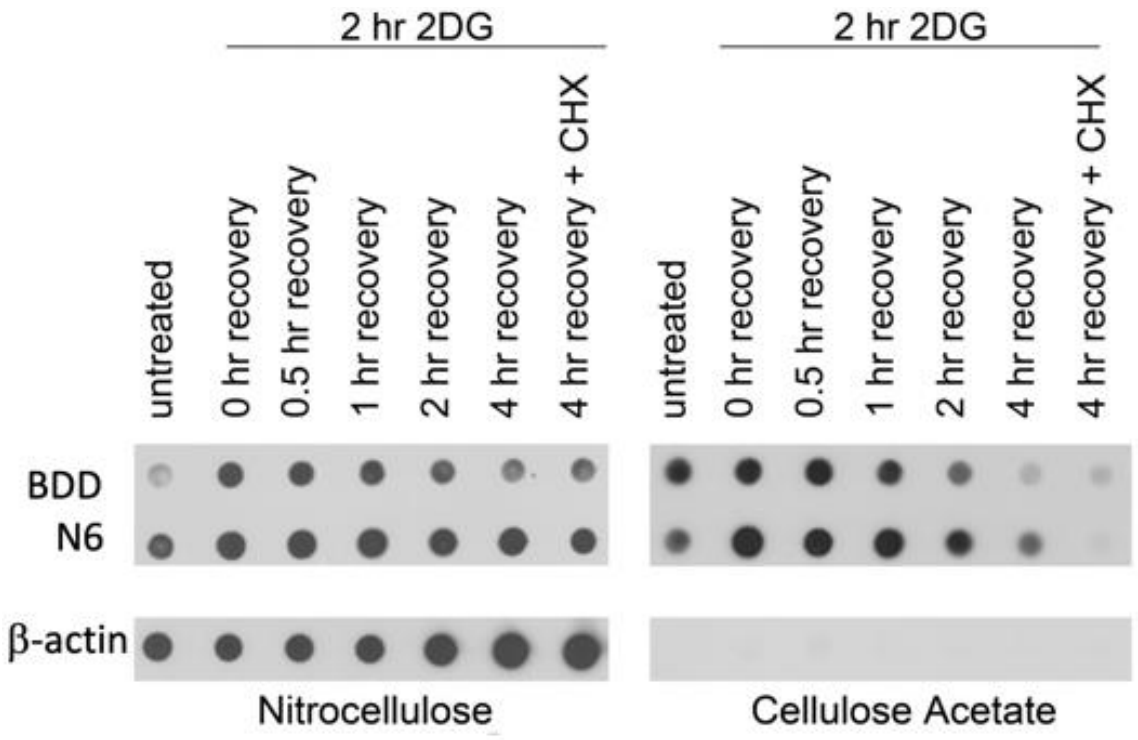

Figure 5. Reversible retention and secretion of active FVIII in CHO cells
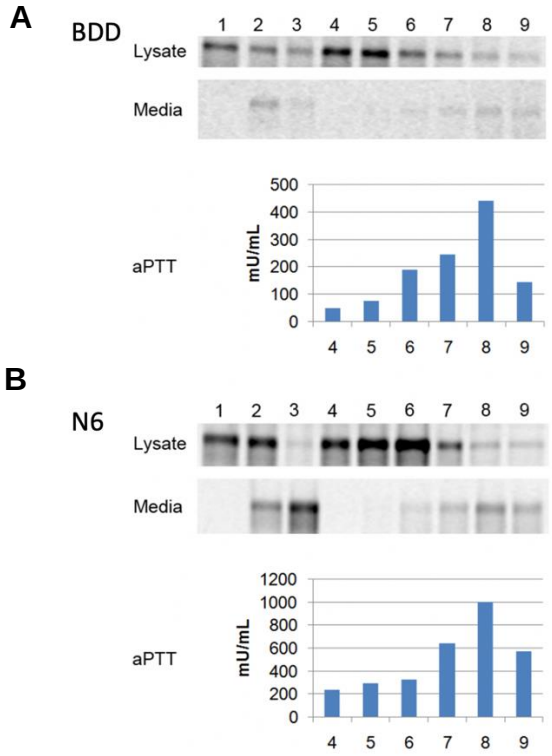
Pulse-chase and aPTT analysis of BDD (**A**) and 226/N6 (**B**). CHO cells were pulse-labeled for 20 min with [^{35}S] met/cys, and then chased for 20 min with media containing excess unlabeled met/cys to complete synthesis of nascent chains (lane 1) before being treated with either normal media (lanes 2-3) or glucose-free media containing 10 mM 2DG and 20 mM NaN3. After 2 hr, cells were harvested (lane 4) or allowed to recover in complete media for increasing times (lanes 5-8), or complete media with CHX (lane 9). 2hr treatment with 2DG followed by recovery in normal media. Lysates and media were collected at indicated time points for FVIII immunoprecipitation and SDS-PAGE. Cells were treated in parallel, but not pulse-labeled, for aPTT activity assay of FVIII in the media. Lanes: 1: Untreated, 20' chase; 2: Untreated 120' chase; 3: Untreated 240' chase; 4-9: 2DG for 120'; 5: 2-DG + 30' recovery; 6: 2-DG + 60' recovery; 7: 2DG + 120' recovery; 8: 2DG + 240' recovery; 9: 2DG + 240' recovery.